

TotalVibeSegmentator: Full Torso Segmentation for the NAKO and UK Biobank in Volumetric Interpolated Breath-hold Examination Body Images

- Robert Graf* (1,2)
- Paul-Sören Platzek (1)
- Evamaria Olga Riedel (1)
- Constanze Ramschütz (1)
- Sophie Starck (2)
- Hendrik Kristian Möller (1,2)
- Matan Atad (1,2)
- Henry Völzke (4)
- Robin Bülow (3)
- Carsten Oliver Schmidt (4)
- Julia Rüdibusch (4)
- Matthias Jung (5)
- Marco Reisert (5)
- Jakob Weiss (5)
- Maximilian Löffler (5)
- Fabian Bamberg (5)
- Bene Wiestler (1),
- Johannes C. Paetzold (6)
- Daniel Rueckert (6,2)
- Jan Stefan Kirschke (1)

*First author / corresponding author

1. Department of Diagnostic and Interventional Neuroradiology, School of Medicine, Technical University of Munich, Germany
2. Institut für KI und Informatik in der Medizin, Klinikum rechts der Isar, Technical University of Munich, Germany
3. Institute for Diagnostic Radiology and Neuroradiolog, University Medicine Greifswald, Germany
4. Institut für Community Medicine, Abteilung SHIP-KEF, University Medicine Greifswald, Germany
5. Department of Diagnostic and Interventional Radiology, University Medical Center Freiburg, Faculty of Medicine, University of Freiburg, Hugstetter Str. 55, 79106, Freiburg, Germany
6. Department of Computing, Imperial College London

TotalVibeSegmentator: Full Torso Segmentation for the NAKO and UK Biobank in Volumetric Interpolated Breath-hold Examination Body Images

Abstract

Objectives: To present a publicly available torso segmentation network for large epidemiology datasets on volumetric interpolated breath-hold examination (VIBE) images.

Materials & Methods: We extracted preliminary segmentations from TotalSegmentator, spine, and body composition networks for VIBE images, then improved them iteratively and retrained a nnUNet network. Using subsets of NAKO (85 subjects) and UK Biobank (16 subjects), we evaluated with Dice-score on a holdout set (12 subjects) and existing organ segmentation approach (1000 subjects), generating 71 semantic segmentation types for VIBE images. We provide an additional network for the vertebra segments 22 individual vertebra types.

Results: We achieved an average Dice score of 0.89 ± 0.07 overall 71 segmentation labels. We scored > 0.90 Dice-score on the abdominal organs except for the pancreas with a Dice of 0.70.

Conclusion: Our work offers a detailed and refined publicly available full torso segmentation on VIBE images.

Keywords:

Deep Learning, Segmentation, Torso

Introduction



Figure 1: 3D rendering of our segmentations for NAKO and UKBB subjects on Volumetric Interpolated Breath-hold Examination (VIBE) water image. A) bones, intervertebral disc, and costal cartilages; B) digestion; C) lung-lobes, and trachea; D) muscles; E) organs; F) vessels; G) spinal cord and canal; H) subcutaneous fat, muscle (other) and inner fat.

Segmentation for MRI is crucial for both clinical purposes and epidemiological studies. Clinically, it may aid in streamlining diagnosis, treatment planning, and personalized healthcare. In epidemiological research, segmentation enables large-scale analysis of

population health, facilitating the computation of crucial health parameters across diverse demographics [1].

The Volumetric Interpolated Breath-hold Examination (VIBE) employs a two-point Dixon sequence to separate water and fat content in MRI images [2]. Large epidemiological studies in Europe, such as the German National Cohort (NAKO) [3], the UK-Biobank (UKBB) [4], and the Study of Health in Pomerania (SHIP) [5] have utilized VIBE for comprehensive torso imaging. Both UKBB and NAKO datasets feature full torso images, with only the head and parts of the arms and legs outside the field of view (FOV).

Recent advancements, such as the release of TotalSegmentator[6], have provided comprehensive torso segmentation for CT scans, promising significant benefits for future research [6]. We extended this segmentation capability to VIBE MR images, enabling the automated evaluation of large full-body image collections from NAKO and UKBB. Our approach combines recent works in spine segmentation in MRI [7–9], domain adaptation to use the TotalSegmentator [6] on MR images, and existing MR-specific annotations by Jung et al. [Under Submission]. The resulting portfolio of regions encompasses 71 distinct semantic segmentation classes plus 22 instance vertebra classes (C3 to L5). By automating the segmentation of these diverse anatomical structures, we aim to provide a robust tool for both clinical applications and large-scale epidemiological research, facilitating the extraction of meaningful biomarkers and the advancement of AI-based reporting and analysis tools, such as early cancer detection [10, 11]. Our segmentations aim to closely produce the same semantic labels as TotalSegmentator, enabling structural comparison between CT and MR images of the same subject. Given that NAKO consists of different anatomically aligned images, our approach can be easily extended to other MR contrasts. This includes T2-weighted HASTE (torso), proton density (hip area), six-point Dixon technique (lower torso), and sagittal T2-weighted turbo spin echo (spine only). We support the open-source mission of TotalSegmentator and freely publish our trained nnUNet [12] weights:

(Github <https://github.com/robert-graf/TotalVibeSegmentator>).

Materials and Methods

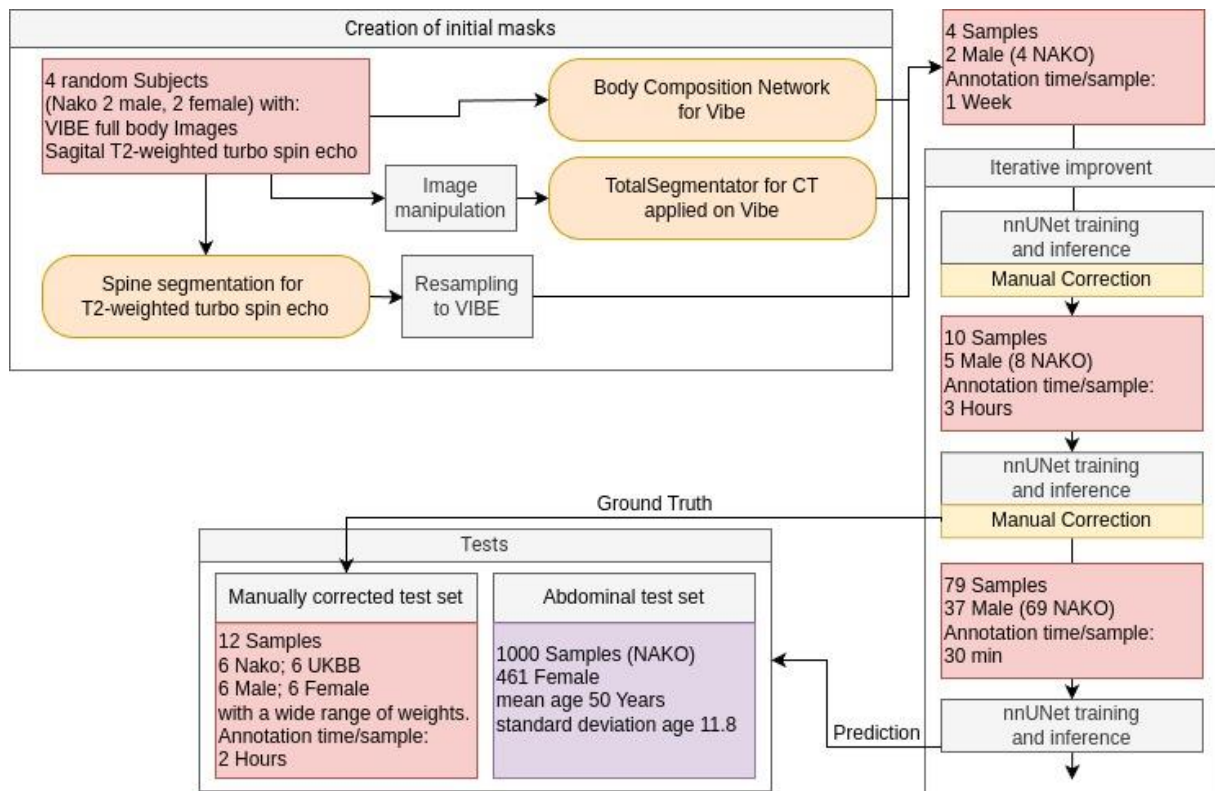


Figure 2: We generate initial masks from different sources (light orange) and then iteratively increase the training dataset. We generate two test sets: A manually corrected test set and a large automatic test set from abdominal organ segmentation. VIBE -Volumetric Interpolated Breath-hold Examination

Data

This study uses a random subset of the full-body VIBE data from NAKO, acquired at Augsburg and Neubrandenburg, along with data from UKBB for training and evaluation. Ethical approval for data collection was obtained from the respective ethics committees, and informed consent was obtained. This prospective data was collected for multiple studies, including the present one. Additionally, ethical approval was obtained from our local ethics committee for this study's content.

The NAKO VIBE images were acquired in four stacks in axial orientation, with an in-plane resolution of 1.4 mm and a through-plane resolution of 3 mm [3]. In comparison, the UKBB VIBE images were obtained with a lower in-plane resolution of 2.2 mm and 3 mm slice thickness [4]. Our network was trained on the native resolution of the NAKO images, with the

UKBB images upscaled to match this resolution. NAKO images were stitched using an in-house tool¹, while UKBB images were stitched using the stitching tool from Glocker et al. [13].

Segmentations

Our final segmentation model included 71 semantic tissue classes, of which two correspond to the bony spine that are further subdivided into up to 22 instance labels (vertebral bodies and posterior elements of C3-L5). The instance labels can be computed separately. In total, we reproduced 84 segmentations that exist in the CT TotalSegmentator version, separated vertebrae in vertebral bodies and posterior elements, and added five additional semantic regions (subcutaneous fat, muscle (other), inner fat, intervertebral disc, and spinal canal).

Due to challenges in annotation, we opted not to segment ribs and merged the colon and small bowel into a single label: "intestine." We found the contrast not strong enough to confidently delineate them in VIBE images for both classes. Skull and brain segmentation are omitted because they fall outside of the field of view (FOV). Additionally, we believe there are already enough well-established algorithms available for skull segmentation in MRI [14, 15]. Additionally, structures like the patella, fibula, tibia, ulna, and radius are seldom and only partially captured in the FOV of the NAKO and UKBB datasets, hence categorized into a collective class labeled "bone (other)." We did not reproduce the cysts classes as we think pathologies are out of scope for this work and are highly underrepresented in UKBB and NAKO compared to a clinical dataset.

In total, we only miss 4 class types that are segmented in the publicly available TotalSegmentator (version 2): ribs, brain, skull, and kidney cysts classes.

¹ We made this tool freely available under <https://github.com/Hendrik-code/TPTBox/tree/main/TPTBox/stitching>. It produces fewer stitching artifacts and is more flexible, but the UKBB images we worked with were already stitched.

Ground truth generation.

As it is unfeasible to annotate full-torso images completely manually to obtain a baseline, we took an iterative, stepwise approach, combining available segmentation models with existing ground truth annotations and several iterations of manual refinements (Figure 1). The segmentation refinement process involves four radiologists utilizing ITK-Snap [16]. Three radiologists with 2-3 years of experience conduct the initial segmentation repair under the supervision of a senior radiologist with 22 years of experience. We used three sources for the initial segmentation proposal: The CT TotalSegmentator on manipulated water images, SPINEPS T2w turbo spine echo for vertebra segmentation [7, 8], and body composition network by Jung et al. [Under submission] to segment the additional subcutaneous fat, muscle (other) and inner fat. Existing segmentations helped us to delineate the remaining missing structures more easily.

Segmentation process - Torso Segmentation

For the initial segmentation of four full-torso NAKO images (2 male, 2 female), three segmentation networks are employed. The body composition network from Jung et al. [Under submission] is utilized to segment subcutaneous fat, muscle (general), and body fat. The intermuscular fat tissue was merged with muscle tissue because differentiating between them is out of the scope of this work. We extended the segmentations to also include the arms and legs. Each VIBE consists of four images: in-phase, out-of-phase, water, and fat. TotalSegmentator (public version 2) [6] is used to generate organs, vessels, and specific muscle segmentations on manipulated water images. Given the rough linear correlation between organ water content and CT attenuation, the water images are manipulated to facilitate segmentation by TotalSegmentator. We used the body composition segmentation to reduce the muscle signal by 20 % in the water image; we selected the background and lung in the in-phase image by thresholding and connected component analysis and subtracted these masks with a value of 600 in the water image. Following this approach, most soft tissue could be segmented with only small errors. These values were determined manually to

make the VIBE water image close enough for the segmentation network to not vastly under-segment the lungs, muscles, and liver in the four initial images. Due to signal shifts, these metrics are not generally applicable to all water images. This process could not produce certain structures such as bone, colon, portal and splenic vein, thyroid gland, spinal cord, and costal cartilage, which were manually segmented. Spine segmentation is derived from aligned T2w sagittal images with SPINEPS [7, 8], resampled to match the VIBE.

After obtaining the first 4 segmentations, we iteratively trained a nnUNet [12], repaired an increasing number of images, and slowly introduced the UKBB images. First 10 (5 male; 8 Nako/2 UKBB), then 79 (37 male, 10 UKBB).

Training the nnUNet

Other papers [6, 8, 17] noted a left-right structure issue with nnUNet [12]. To address this swapping in our nnUNet training, we implement several strategies. Firstly, we turn off random flipping during training. Additionally, we augment the patch window in the in-plane resolution to expand the field of view (FOV) to 224 pixels (315 mm) and 64 pixels (192 mm) in through-plane resolution. To aid the network in locating its approximate position, we segment the body into eleven quadrants (Figure 8) on a downscaled 4 mm isometric image with a large FOV (96 pixels; 384 mm in all directions)

Moreover, we employ elastic deformation [18] to generate additional training images, increasing the dataset size by a factor of 500. We utilized an iterative approach similar to TotalSegmentator [6] and AbdomenAtlas-8K [19] to increase the number of training images. This iterative process involves repairing predicted segmentation masks and retraining the network until achieving a point of diminishing returns.

The segmentation model is trained on a single input image out of water, in-phase, or out-of-phase contrast. For new training segmentations of the three inputs were merged into a single image. We remove connected components smaller than a specific volume threshold for each organ. If an organ only consists of one tightly packed connected component, we discard all components except the largest. Prioritization during merging focuses on structures prone to

under-segmentation, with lower priority segmentations only added to unoccupied voxels. This computer-intensive process aids in eliminating small false positives and underpredictions, particularly for vessels. With the model trained on 79 or more subjects, this step is no longer needed to prevent common under-segmentation. We have rewritten the inference code of nnUNet. The large number of classes and image size lead to a considerable slowdown in the original implementation. The rewritten code frees the GPU memory earlier and is faster.

Segmentation Process – Other Image Contrasts

To increase generalizability, we resampled other sequences available in NAKO, such as T2w haste (torso), proton density (pelvis), 6-point Dixon (lower torso), and sagittal T2w turbo spin echo (spine) to the spacing of the VIBE images to 1.4 mm in the axial plane and 3 mm in the superior-inferior direction. We manually removed all samples with motion artifacts. The remaining sequences were used for training after we achieved ten corrected subjects.

Segmentation Process – Spine

For the spine, we use aligned T2-weighted turbo spin echo images with the VIBE. Instance labels were defined by counting from the neck downwards in the T2-weighted images. For training, we resampled 2000 instance segmentations from T2-weighted turbo spin echo to VIBE. The predictions from the resulting segmentation model eliminated step-shape interpolation errors and appeared more accurate than the original training data (see Figure 7). We omitted an evaluation for three reasons: this serves as a stopgap for users interested in the rough location of the vertebra level, we currently have no ground truth for spine segmentation on vibe, and we plan to provide models for the SPINEPS [7, 8] approach in a future release, which will reduce the risk of off-by-one errors and vertebra merging.

Evaluations

For external validation, we utilize the inference of the abdominal networks as outlined in Kart et al. [20]. We validate our model on 12 manually corrected images, evenly distributed between NAKO and UKBB datasets (50% male), selected to cover a wide range of body

weights per sex and dataset. Quality metrics are assessed using the Dice score. We report the average symmetric surface distance in Supplement Figure 9.

Statistical Analysis

For evaluation, we utilize the Scipy [21] and Panoptica Python [19] packages. Nonparametric bootstrapping of 10,000 iterations is utilized to compute 95% confidence intervals (CIs).

Results

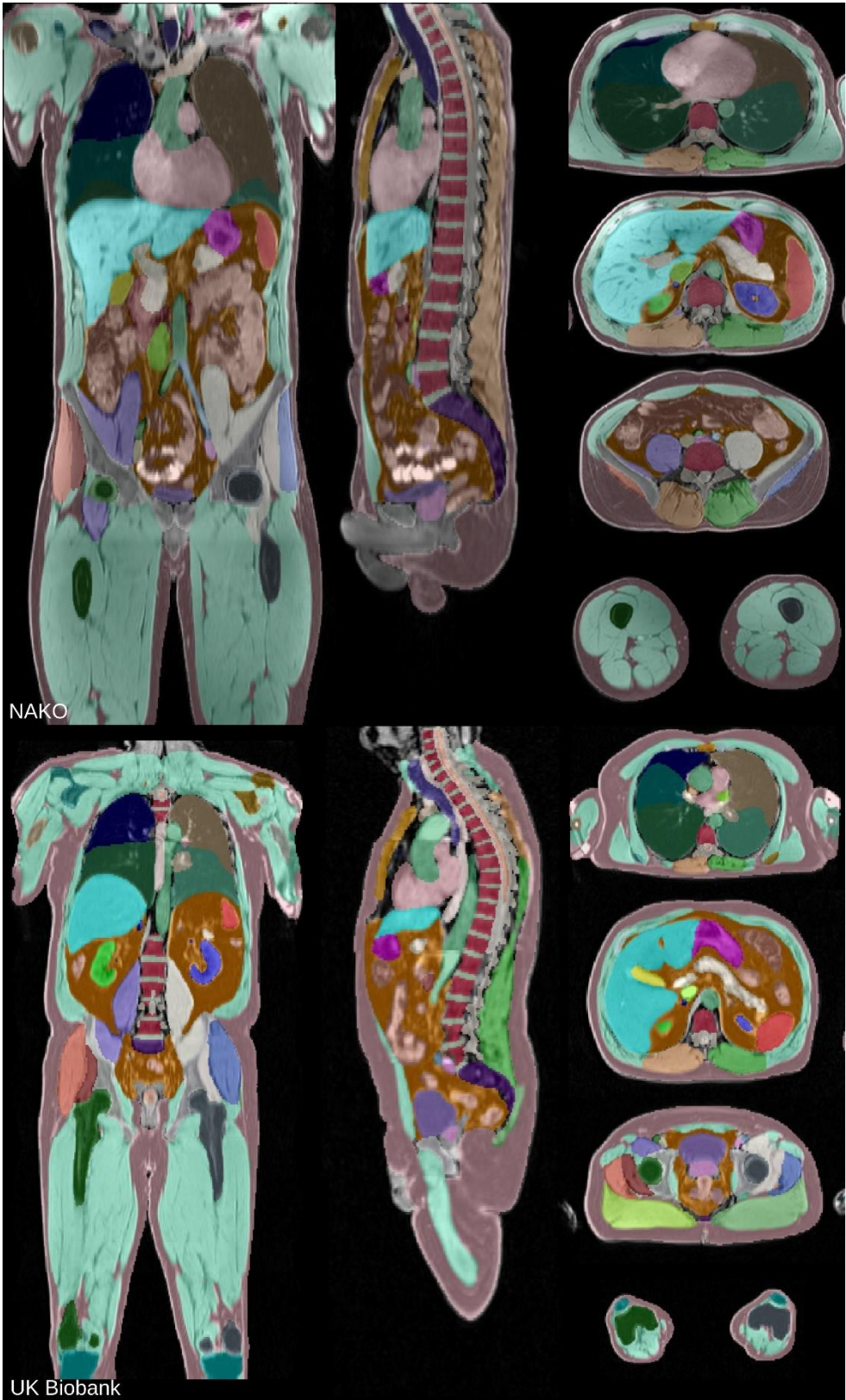


Figure 3: Segmentation for two random Volumetric Interpolated Breath-hold Examination (VIBE) images on the NAKO and UK Biobank.

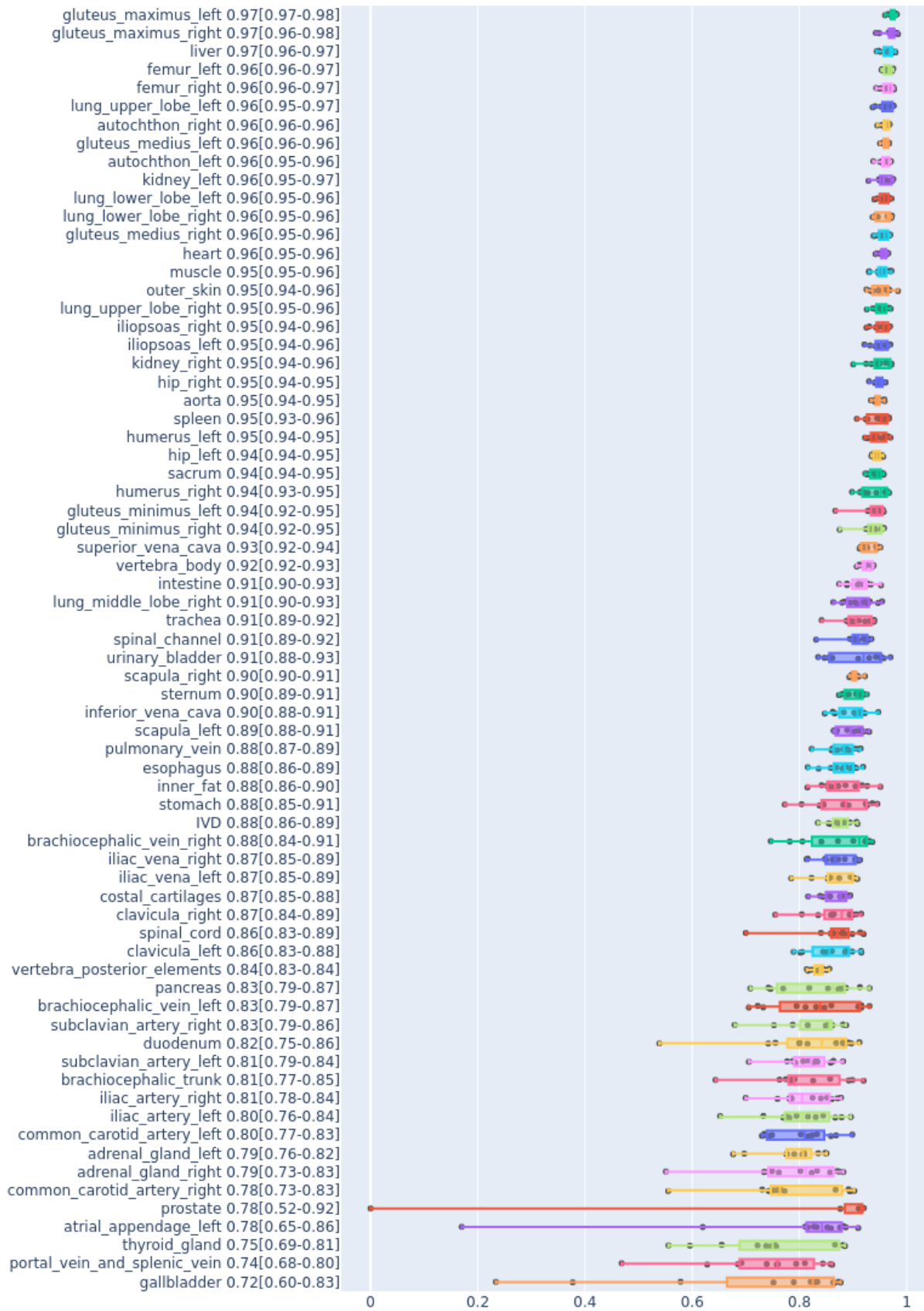


Figure 4: Dice-scores over all classes compared on repaired and predicted Volumetric Interpolated Breath-hold Examination (VIBE) on the 12 NAKO and UK Biobank images.

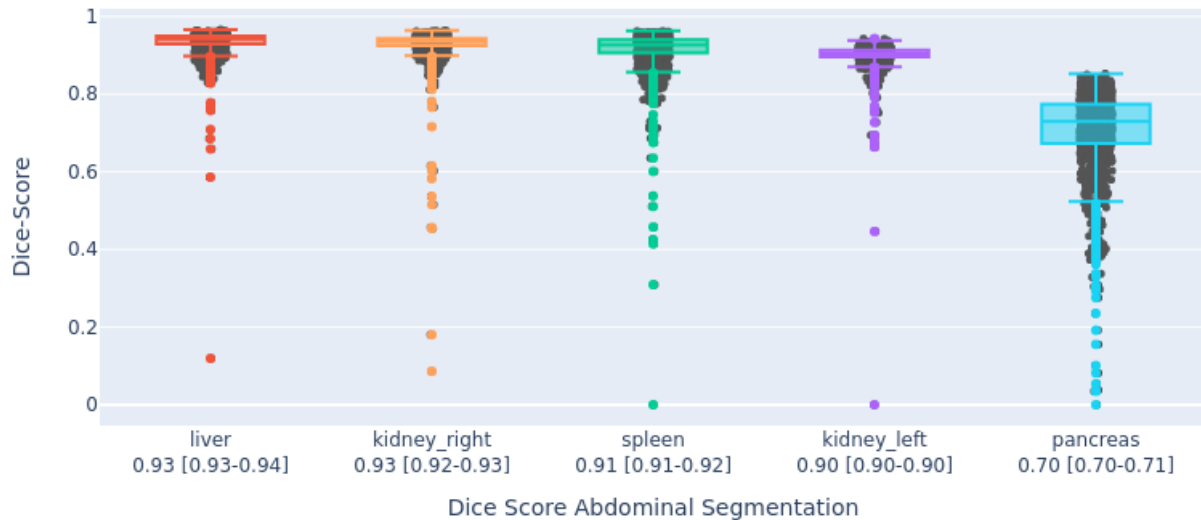


Figure 5: Dice-scores over 1000 test samples compared to the prediction of the NAKO/UKBB abdomen segmentation network. Although without manual reference masks, this shows the agreement between both approaches. The source of outliers can be caused by either of the networks.

On our internal test set, the average Dice-Score is 0.89 ± 0.07 over all classes. Thyroid gland, gallbladder and “portal vein and splenic vein” are the lowest Dice score, due to the low contrast in Vibe. Our model sometimes predicts a prostate in female subjects, causing a Dice-Score of 0. Individual Scores are in Figure 4.

Our segmentation closely aligns with abdominal segmentation [20] for the liver, kidney, and spleen (see Figure 5). The pancreas, however, presents challenges in achieving consistent segmentation, leading to discrepancies in its outline, as also reported by Kart et al. [20]. Figure 6 demonstrates the capabilities of additional NAKO sequence types. Figure 7 presents our segmentation of the spine. As previously noted in the literature [6, 8, 23], this method is prone to instability, resulting in vertebra labels being offset by one, and occasionally, a single vertebra is labeled as two different vertebra ids, dividing it.

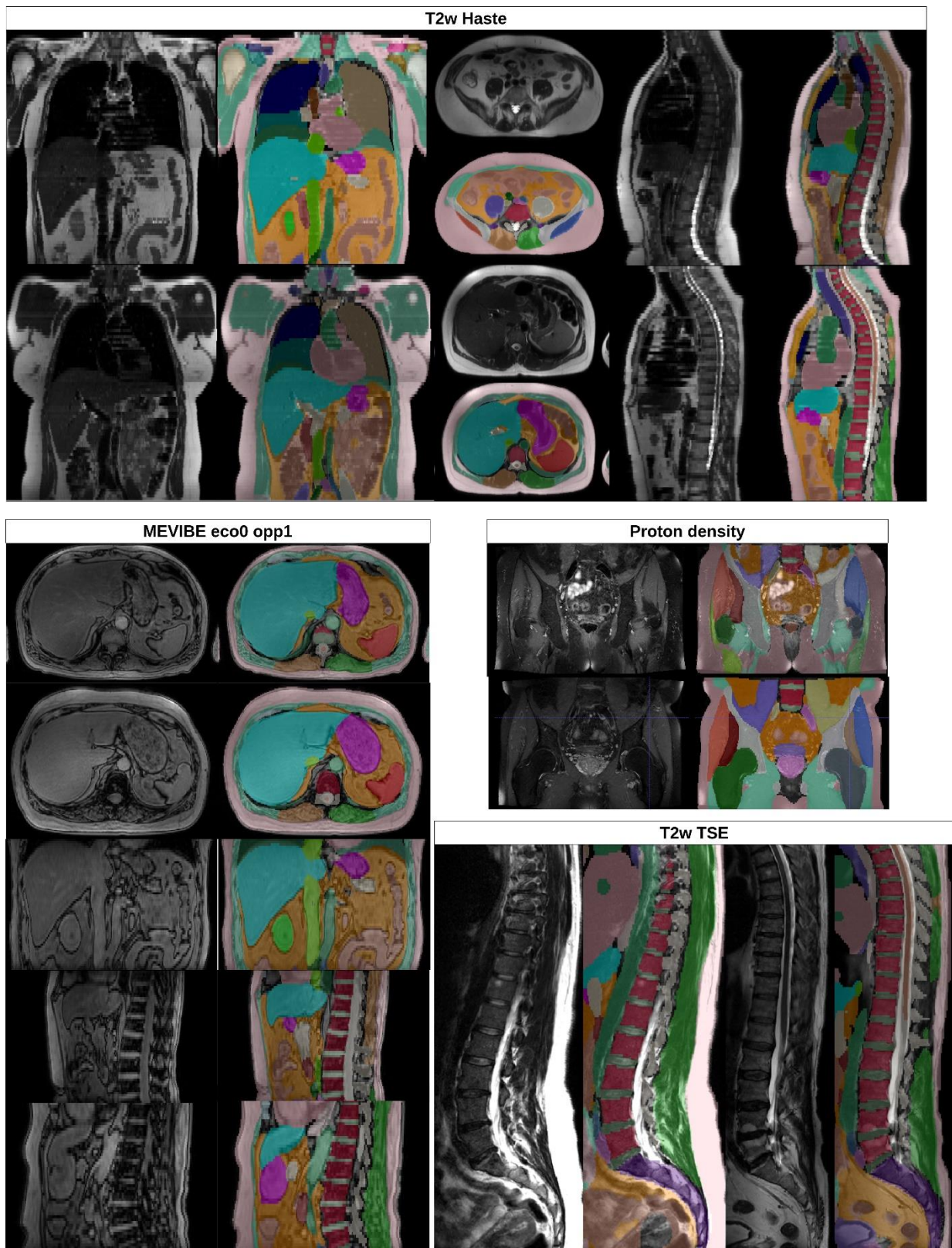


Figure 6: Running our segmentation on other NAKO sequence types. We used for training resampled ground truth segmentation to the other sequences. T2w Haste (Half Fourier-acquisition single-shot turbo spin echo) works best even with the breathing and heart movement of the images. MEVIBE (multi echo vibe) has out of phase images with clear delineations like the “eco0 opp1” signal. The proton density and T2w TSE (turbo spin echo) has signal drops in the NAKO, producing errors where the signal drop is too strong.

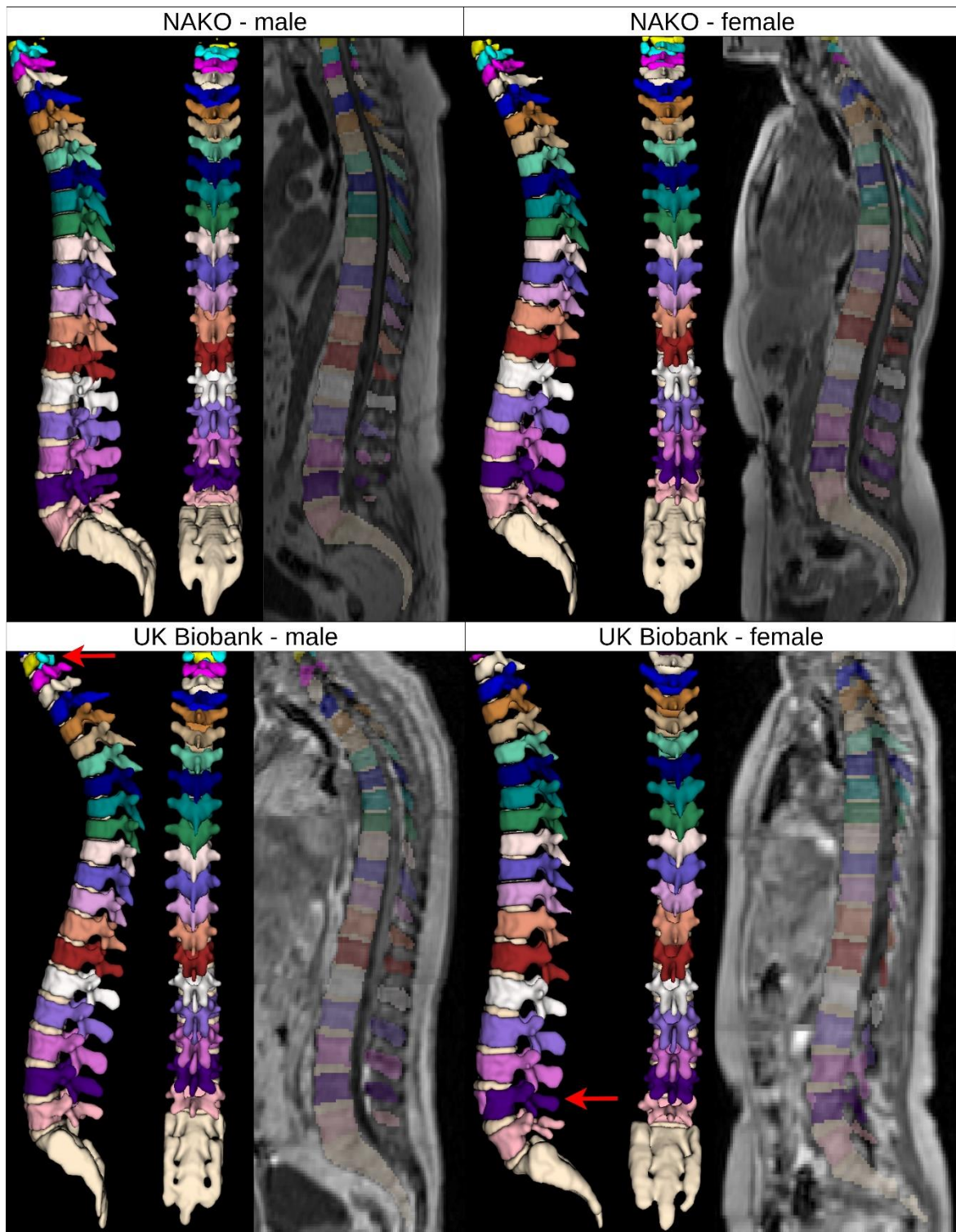


Figure 7: Spine instance segmentation. One the NAKO vibs off-by-one errors are rare. For out-of-distribution like the UKBB vertebra merging and off-by-one errors are common. We marked two examples with a red arrow.

Discussion

In this study, we developed a comprehensive, full torso segmentation model with 71 semantic segmentation labels and additional vertebra instance segmentation for the NAKO and UKBB VIBE images. Next to 20 organs, 10 muscles, 19 vessels, 16 bones, and 3 others (Intervertebral disc, spinal cord and spinal canal), we also include a segmentation of the body composition (3 classes), i.e. different fat compartments and body parts. Our approach was enhanced by training on additional sequence types, allowing for improved refinement across diverse datasets. As in CT, MRI total segmentation on VIBE images holds significant potential in medical imaging, providing detailed anatomical insights and facilitating advanced research [6]. Previous studies have shown the effectiveness of segmentation techniques in the NAKO cohort, such as abdominal organ segmentation and quality control in a large sample of 20,000 participants [20]. Our model provides extended segmented fat, subcutaneous fat, and muscle tissues based on Jung et al. [Under submission] on Vibe. Such segmentation can be used to estimate fat distribution like by Somasundaram and Wu et al. applied to 6-point Dixon images [24].

Comparative studies include "MRISegmentator-Abdomen," [25] a fully automated tool for multi-organ and structure segmentation in T1-weighted abdominal MRI, achieving 33 semantic segmentations, 11 spine instance segmentations, and 18 rib instance segmentations. Another paper called "MRSegmentator" [17] claims robust multi-modality segmentation across 40 classes in both MRI and CT sequences. These papers highlight the growing advancements in MRI segmentation. We expect multiple multi-segmentation models to be released in the near future. This provides the scientific community with independent bases for abdominal segmentation across different modalities, enabling cross-validation and strengthening the robustness of segmentation techniques. Our ground truth was developed independently and has the most segmentation types in MRI so far. These independent developments present an opportunity for valuable comparative analysis.

Despite its advantages, the NAKO dataset presents certain limitations. While it offers a large field of view (FOV) and high resolution, it contains fewer anomalies, which might limit the diversity of pathological cases in the training data. We omitted pathology segmentation as they are out of the scope of this work. We need to increase the training set size to show the network more variation, including common pathologies. For the digestive organs, we observe that delineation is more difficult in Vibe than in T1-weighted fast spin echo images with a contrast agent, as there is barely a contrast change in Vibe, unlike in contrast-enhanced images. The availability of HASTE, PD, and MEVIBE sequences for free is a notable benefit, but challenges remain. For instance, very small structures in the UKBB dataset, such as the thyroid gland, are difficult to segment due to being nearly lost in the image noise. Additionally, the arms, legs and head are only partially visible in all datasets. The segmentation behavior on these structures is undefined and requires a separate improvement dataset. From the feedback of other radiologists, we know that our sacrum includes non-bone tissue, and our thyroid gland follows delineation that is visible in VIBE MRI, but the 3D view shows that this leads to another segmentation than in CT.

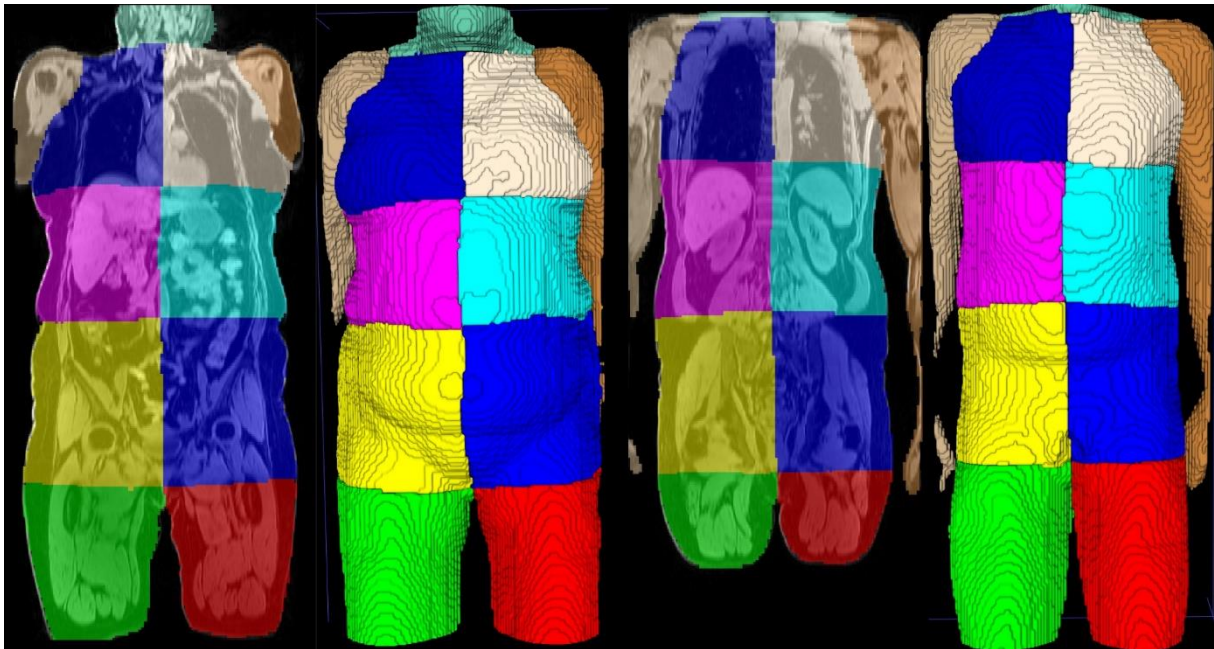
The TotalSegmentator [6] and SPINEPS [7, 8] papers highlight nnUNet's [12] patch-wise inference limitations, which can cause off-by-one errors and vertebra merging, making it less suitable for instance segmentation. Moreover, adding approximately 25 vertebra classes increases the system requirements to run the algorithm. Despite these challenges, fast instance segmentation remains valuable for researchers and medical professionals. To address this, we trained a separate instance network, where we expect these issues to remain. In the future, these issues can be solved by specialized networks. SPINEPS [8] already solves the merging issue with its two-step approach but cannot yet label the vertebra to their class and naively counts from top to bottom.

Exploring better approaches than nnU-Net and extending the segmentation to other modalities are potential areas for future research. Further work could involve merging or managing the model zoo of total MRI segmentation through federated learning, enhancing

the generalizability and applicability of segmentation models across various datasets and modalities that will be released in the future.

In conclusion, our work significantly contributes to the field of MRI segmentation, offering a detailed and refined approach to full torso segmentation. By addressing the limitations and exploring to overcome existing issues like right-left miss segmentation, we aim to advance the capabilities of MRI segmentation and support its application in diverse clinical and research settings.

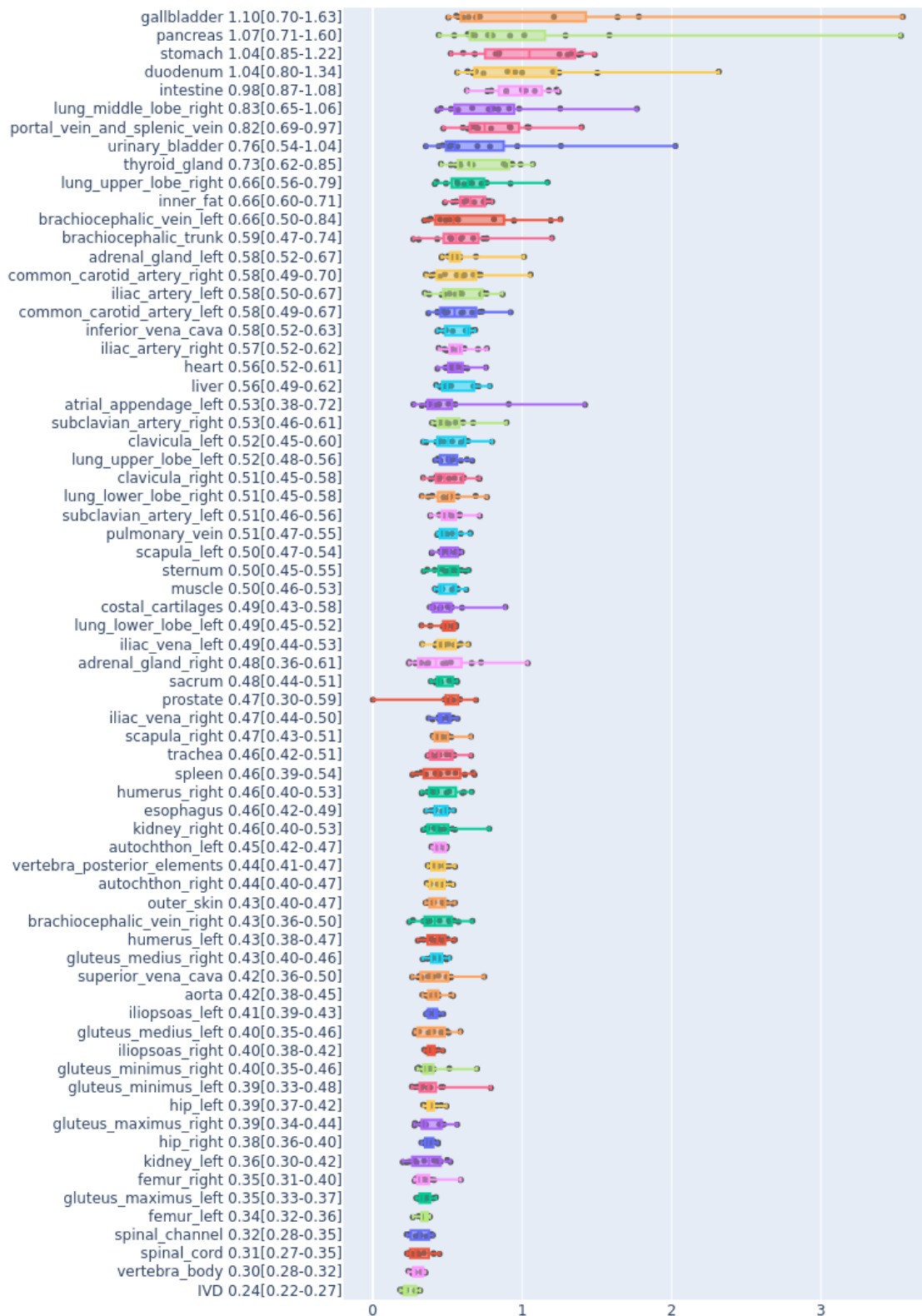
Supplements



Supplement Figure 8: The “eleven quadrants” segmentation on two examples from the NAKO. It is segmented on 4 mm isometric images and is used as an additional input for the TotalVibeSegmentator.

Supplement Table 1: List of classes in our TotalVibeSegmentator and the public facing TotalSegmentator (version 2) for CT images.

TotalSegmentator name	Chirality/Instances	Difference + Reasoning
Spleen		
Kidney	Left, Right	
Gallbladder		
Liver		
Stomach		
Pancreas		
Adrenal gland	Left, Right	
Lung upper lobe	Left, Right	
Lung lower lobe	Left, Right	
Lung middle lobe right		
Esophagus		
Trachea		
Thyroid gland		
Small bowel		Merged with small colon; Now: Intestine
Duodenum		
Colon		Merged with small bowel; Now: Intestine
Urinary bladder		
Prostate		
Kidney cyst	Left, Right	Missing; Out of scope for this work
Sacrum		
Vertebrae	C1-C7, T1-T12, L1-L5, S1	Replaced by vertebra body and vertebra posterior elements
Heart		
Aorta		
Pulmonary vein		
Brachiocephalic trunk		
Subclavian artery	Left, Right	
Common carotid artery	Left, Right	
Brachiocephalic vein	Left, Right	
Atrial appendage left		
Superior vena cava		
Inferior vena cava		
Portal vein and splenic vein		
Iliac artery	Left, Right	
Iliac vena	Left, Right	
Humerus	Left, Right	
Scapula	Left, Right	
Clavicula	Left, Right	
Femur	Left, Right	
Hip	Left, Right	
Spinal cord		
Gluteus maximus	Left, Right	
Gluteus medius	Left, Right	
Gluteus minimus	Left, Right	
Autochthon	Left, Right	
Iliopsoas	Left, Right	
Brain		Missing; Outside FOV
Skull		Missing; Outside FOV
Rib	[Left, Right] x [1 - 12]	Missing; Not reproduced due to time constrains
Sternum		
Costal artilages		
Outer skin		New in TotalVibeSegmentator
Muscle (other)		New in TotalVibeSegmentator
Inner fat		New in TotalVibeSegmentator
IVD		New in TotalVibeSegmentator
Vertebra body		New in TotalVibeSegmentator
Vertebra posterior elements		New in TotalVibeSegmentator
Spinal channel		New in TotalVibeSegmentator
Bone (other)		New in TotalVibeSegmentator



Supplement Figure 9: Average Symmetric Surface Distance in mm (lower is better) over all classes compared on repaired and predicted Volumetric Interpolated Breath-hold Examination (VIBE) on the 12 NAKO and UK Biobank images.

References

1. Gillies RJ, Kinahan PE, Hricak H (2016) Radiomics: images are more than pictures, they are data. *Radiology* 278:563–577
2. Koh E, Walton ER, Watson P (2018) VIBE MRI: an alternative to CT in the imaging of sports-related osseous pathology? *The British Journal of Radiology* 91:20170815
3. Bamberg F, Kauczor H-U, Weckbach S, et al (2015) Whole-body MR imaging in the German National Cohort: rationale, design, and technical background. *Radiology* 277:206–220. <https://doi.org/10.1148/radiol.2015142272>
4. Allen N, Sudlow C, Downey P, et al (2012) UK Biobank: Current status and what it means for epidemiology. *Health Policy Technol (HPT)* 1:123–126. <https://doi.org/10.1016/j.hlpt.2012.07.003>
5. John U, Hensel E, Lüdemann J, et al (2001) Study of Health In Pomerania (SHIP): a health examination survey in an east German region: objectives and design. *Sozial-und Präventivmedizin* 46:186–194
6. Wasserthal J, Breit H-C, Meyer MT, et al (2023) Totalsegmentator: Robust segmentation of 104 anatomic structures in ct images. *Radiology: Artificial Intelligence* 5:
7. Graf R, Schmitt J, Schlaeger S, et al (2023) Denoising diffusion-based MRI to CT image translation enables automated spinal segmentation. *European Radiology Experimental* 7:70. <https://doi.org/10.1186/s41747-023-00385-2>
8. Möller H, Graf R, Schmitt J, et al (2024) SPINEPS—Automatic Whole Spine Segmentation of T2-weighted MR images using a Two-Phase Approach to Multi-class Semantic and Instance Segmentation. *arXiv preprint arXiv:240216368*
9. Streckenbach F, Leifert G, Beyer T, et al (2022) Application of a Deep Learning Approach to Analyze Large-Scale MRI Data of the Spine. In: *Healthcare*. MDPI, p 2132
10. Mikdadi D, O’Connell KA, Meacham PJ, et al (2022) Applications of artificial intelligence (AI) in ovarian cancer, pancreatic cancer, and image biomarker discovery. *Cancer Biomarkers* 33:173–184
11. Prelaj A, Miskovic V, Zanitti M, et al (2023) Artificial intelligence for predictive biomarker discovery in immuno-oncology: A systematic review. *Annals of Oncology*
12. Isensee F, Jaeger PF, Kohl SA, et al (2021) nnU-Net: a self-configuring method for deep learning-based biomedical image segmentation. *Nature methods* 18:203–211
13. Glocker B, Wachinger C, Zeltner J, et al (2009) MRI composing for whole body imaging. In: *Bildverarbeitung für die Medizin 2009: Algorithmen—Systeme—Anwendungen Proceedings des Workshops vom 22. bis 25. März 2009 in Heidelberg*. Springer, pp 420–424

14. Reuter M, Schmansky NJ, Rosas HD, Fischl B (2012) Within-subject template estimation for unbiased longitudinal image analysis. *Neuroimage* 61:1402–1418
15. Akkus Z, Galimzianova A, Hoogi A, et al (2017) Deep learning for brain MRI segmentation: state of the art and future directions. *Journal of digital imaging* 30:449–459
16. Yushkevich PA, Piven J, Cody Hazlett H, et al (2006) User-Guided 3D Active Contour Segmentation of Anatomical Structures: Significantly Improved Efficiency and Reliability. *Neuroimage* 31:1116–1128
17. Häntze H, Xu L, Dorfner FJ, et al (2024) MRSegmentator: Robust Multi-Modality Segmentation of 40 Classes in MRI and CT Sequences. *arXiv preprint arXiv:240506463*
18. Ronneberger O, Fischer P, Brox T (2015) U-net: Convolutional networks for biomedical image segmentation. In: *Medical Image Computing and Computer-Assisted Intervention--MICCAI 2015: 18th International Conference*. Springer, pp 234-241. https://doi.org/10.1007/978-3-319-24574-4_28
19. Qu C, Zhang T, Qiao H, et al (2024) Abdomenatlas-8k: Annotating 8,000 CT volumes for multi-organ segmentation in three weeks. *Advances in Neural Information Processing Systems* 36:
20. Kart T, Fischer M, Winzeck S, et al (2022) Automated imaging-based abdominal organ segmentation and quality control in 20,000 participants of the UK Biobank and German National Cohort Studies. *Scientific Reports* 12:18733
21. Virtanen P, Gommers R, Oliphant TE, et al (2020) SciPy 1.0: fundamental algorithms for scientific computing in Python. *Nature methods* 17:261–272
22. Kofler F, Möller H, Buchner JA, et al (2023) Panoptica – instance-wise evaluation of 3D semantic and instance segmentation maps
23. van der Graaf JW, van Hooff ML, Buckens CF, et al (2024) Lumbar spine segmentation in MR images: a dataset and a public benchmark. *Scientific Data* 11:264
24. Somasundaram A, Wu M, Reik A, et al Evaluating Sex-specific Differences in Abdominal Fat Volume and Proton Density Fat Fraction on MRI Scans Using Automated nnU-Net-based Segmentation. *Radiology: Artificial Intelligence* 0:e230471. <https://doi.org/10.1148/ryai.230471>
25. Zhuang Y, Mathai TS, Mukherjee P, et al (2024) MRISegmentator-Abdomen: A Fully Automated Multi-Organ and Structure Segmentation Tool for T1-weighted Abdominal MRI. *arXiv preprint arXiv:240505944*

Declarations

Ethics approval and consent to participate

The ethics committee of the Technical University Munich approved this retrospective, German-law-compliant study (593/21 S-NP) and waived the need for informed consent.

Availability of data and materials

The models are freely available under: (Github, <https://github.com/robert-graf/TotalVibeSegmentator>)

The datasets used and/or analyzed during the current study are available from the corresponding author on reasonable request. The NAKO, UKBB and SHIP are available through third parties upon application.

Competing interests

J. S. K are Cofounders and shareholders of Bonescreen GmbH. See <https://bonescreen.de/>.

The authors who analyzed and controlled the data are not employees, cofounders, or shareholders of Bonescreen GmbH.

Funding

The research for this article received funding from the European Research Council (ERC) under the European Union's Horizon 2020 research and innovation program (101045128—iBack-epic—ERC2021-COG).

This project was conducted with data from the German National Cohort (GNC) (www.nako.de). The GNC is funded by the Federal Ministry of Education and Research (BMBF) [project funding reference numbers: 01ER1301A/B/C and 01ER1511D], federal states and the Helmholtz Association with additional financial support by the participating universities and the institutes of the Leibniz Association. We thank all participants who took part in the GNC study and the staff in this research program.